LETTER

https://doi.org/10.1038/s41586-019-0875-2

Super-Mendelian inheritance mediated by CRISPR–Cas9 in the female mouse germline

Hannah A. Grunwald[1,5], Valentino M. Gantz[1,5], Gunnar Poplawski[2,4,5], Xiang-Ru S. Xu[1], Ethan Bier[1,3] & Kimberly L. Cooper[1,3]*

A gene drive biases the transmission of one of the two copies of a gene such that it is inherited more frequently than by random segregation. Highly efficient gene drive systems have recently been developed in insects, which leverage the sequence-targeted DNA cleavage activity of CRISPR–Cas9 and endogenous homology-directed repair mechanisms to convert heterozygous genotypes to homozygosity[1–4]. If implemented in laboratory rodents, similar systems would enable the rapid assembly of currently impractical genotypes that involve multiple homozygous genes (for example, to model multigenic human diseases). To our knowledge, however, such a system has not yet been demonstrated in mammals. Here we use an active genetic element that encodes a guide RNA, which is embedded in the mouse tyrosinase (*Tyr*) gene, to evaluate whether targeted gene conversion can occur when CRISPR–Cas9 is active in the early embryo or in the developing germline. Although Cas9 efficiently induces double-stranded DNA breaks in the early embryo and male germline, these breaks are not corrected by homology-directed repair. By contrast, Cas9 expression limited to the female germline induces double-stranded breaks that are corrected by homology-directed repair, which copies the active genetic element from the donor to the receiver chromosome and increases its rate of inheritance in the next generation. These results demonstrate the feasibility of CRISPR–Cas9-mediated systems that bias inheritance of desired alleles in mice and that have the potential to transform the use of rodent models in basic and biomedical research.

A cross between mice that are heterozygous for each of three unlinked genes must produce 146 offspring for a 90% probability that one will be a triple homozygous mutant. The likelihood decreases further if any of the three mutations are genetically linked but on opposite homologous chromosomes, because recombination events that combine alleles onto the same chromosome would be very infrequent. The cost, time and requirement for a large number of mice to obtain a few individuals of the desired genotype are therefore prohibitive for certain complex models of multigenic evolutionary traits or human diseases, such as arthritis and cancer.

Recently, CRISPR–Cas9-mediated gene drive systems were developed in *Drosophila* and anopheline mosquitoes that increase the frequency of inheritance of desired alleles[1–4]. These used genetic elements, which we refer to broadly as active genetic elements, that can carry transgenes or orthologous sequences from other species[5]. Notably, an active genetic element includes a guide RNA (gRNA) and is inserted into the genome at the precise location that is targeted for cleavage by the encoded gRNA. In a heterozygous animal that also expresses the Cas9 nuclease, the gRNA targets cleavage of the wild-type homologous chromosome. Genomic sequences that flank the active genetic element then correct the double-stranded break (DSB) by homology-directed repair (HDR), which copies the active genetic element from the donor to the receiver chromosome and converts the heterozygous genotype to homozygosity. The frequency of transmitting the active genetic element to the next generation is therefore greater than expected by random segregation of heterozygous alleles and is referred to as 'super-Mendelian'. In addition to the potential to overcome the obstacles of assembling complex genotypes in laboratory rodents, variations of a CRISPR–Cas9-mediated system have been proposed that might help to suppress invasive rodent populations and/or reduce the prevalence of rodent-borne disease[6,7].

Despite the high efficiency observed in insects, the approximately 790 million years of divergence since their last common ancestor with mammals presents two potential obstacles to the implementation of active genetics in mice; the frequency of DSB formation using a genetically encoded Cas9 and gRNA and/or the frequency of HDR may prevent efficient gene conversion. The alternative DSB repair pathway, non-homologous end joining (NHEJ), frequently generates small insertions and deletions (indels) that make CRISPR–Cas9 an effective means of mutating specific sites in the genome. Although HDR of CRISPR–Cas9-induced DSBs does occur in vitro and in vivo in mammalian cells and embryos, usually from a plasmid or single-stranded DNA template, NHEJ is the predominant mechanism of DSB repair in somatic cells[8,9].

To assess the feasibility of active genetic systems in mice, we designed a 'CopyCat' element[10] that differs from the genetic element used initially in insects in that it cannot self-propagate, because it encodes a gRNA but not the Cas9 protein (Fig. 1a). We designed our strategy to disrupt the tyrosinase gene (*Tyr*), because of the obvious albino phenotype of homozygous loss-of-function mice[11] and to make use of a previously characterized *Tyr* gRNA with high activity[12]. The precise insertion of this element into the gRNA cut site in exon 4 of *Tyr* to obtain the $Tyr^{CopyCat}$ knock-in allele is shown in Extended Data Fig. 1 (see also Supplementary Methods and Supplementary Figs. 1, 2). In brief, the *Tyr* gRNA is transcribed from a constitutive human RNA polymerase III U6 promoter[13]. On the reverse strand of the DNA, to minimize possible transcriptional conflict, mCherry is ubiquitously expressed from the human cytomegalovirus (CMV) immediate-early promoter and enhancer[14]. As the 2.8-kb insert disrupts the *Tyr* open reading frame, $Tyr^{CopyCat}$ is a functionally null (albino) allele that is propagated by Mendelian inheritance in the absence of Cas9. Crossing mice that carry the $Tyr^{CopyCat}$ element to transgenic mice that express Cas9 enabled us to test whether it is possible to observe super-Mendelian inheritance of the $Tyr^{CopyCat}$ allele. For this analysis, we assessed eight different genetic strategies that use existing tools to provide spatial and temporal control of Cas9 expression in the early embryo and in the male and female germlines.

We used two 'constitutive' *cas9* transgenic lines, *Rosa26-cas9*[15] and *H11-cas9*[16], which express Cas9 in all tissues that have been assessed. Each is driven by a ubiquitous promoter and is placed in the respective *Rosa26* or *H11* 'safe harbour' locus. To track the inheritance of the chromosome that is targeted for gene conversion, we bred the *chinchilla* allele of tyrosinase ($Tyr^{c\text{-}ch}$, here simplified to Tyr^{ch}) into each *cas9* transgenic line. Tyr^{ch} encodes a hypomorphic point mutation in exon 5 that is tightly linked to the gRNA target site in exon 4. Tyr^{ch} homozygotes or heterozygotes that also have a null allele have a grey coat colour, and the G to A single-nucleotide polymorphism can be scored with certainty by PCR followed by DNA sequencing[17] (Supplementary Fig. 4).

[1]Division of Biological Sciences, Section of Cellular and Developmental Biology, University of California, San Diego, La Jolla, CA, USA. [2]Department of Neurosciences, University of California, San Diego, La Jolla, CA, USA. [3]Tata Institute for Genetics and Society, University of California, San Diego, La Jolla, CA, USA. [4]Present address: Department of Medicine, National University of Singapore, Singapore, Singapore. [5]These authors contributed equally: Hannah A. Grunwald, Valentino M. Gantz, Gunnar Poplawski. *e-mail: kcooper@ucsd.edu

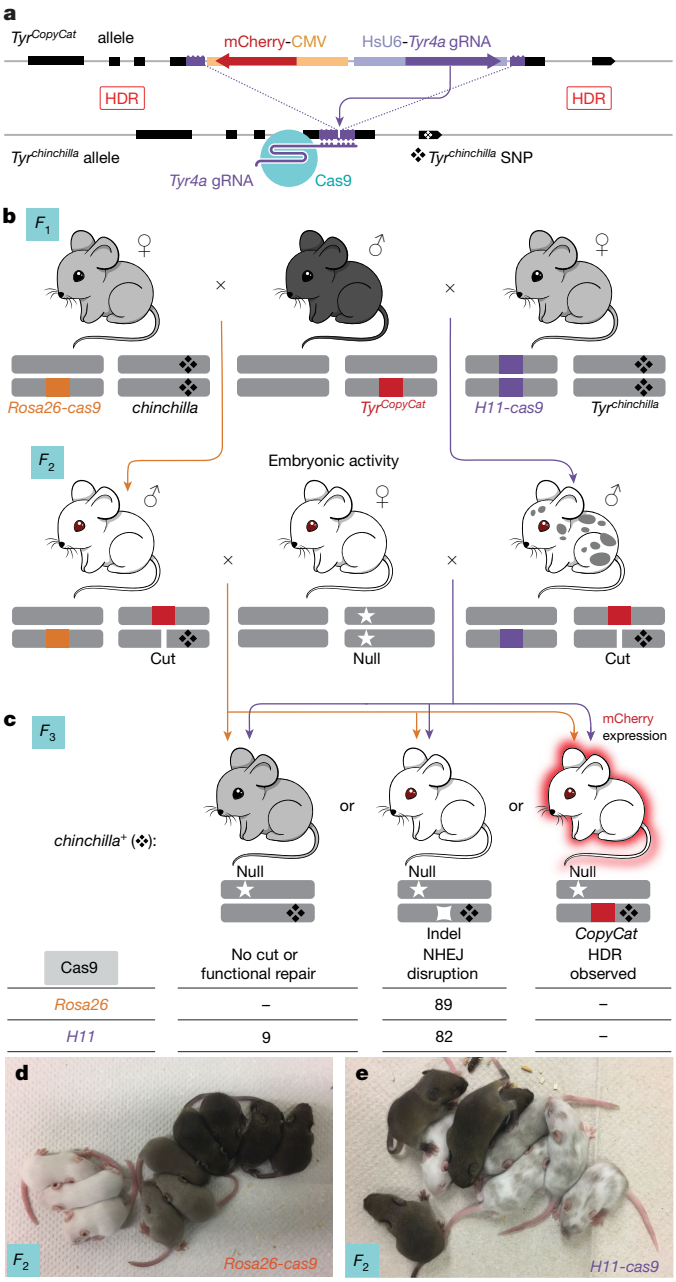

Fig. 1 | Embryonic Cas9 activity does not copy the *Tyr*^{CopyCat} allele from the donor to the receiver chromosome. a, Schematic. The genetically encoded *Tyr*^{CopyCat} element, when combined with a transgenic source of Cas9, is expected to induce a DSB in the *Tyr*^{ch}-marked receiver chromosome, which could be repaired by inter-homologue HDR. **b**, Breeding strategy to combine *Tyr*^{CopyCat} with a constitutive *cas9* transgene followed by a cross between *Tyr*^{CopyCat} and *Tyr*^{null} mice. **c**, Summary of the F_3 cross offspring of five independent families for each *Rosa26-cas9* and *H11-cas9* genotype. **d**, A representative litter of six *Rosa26-cas9* F_2 litters. Black mice did not inherit *Tyr*^{CopyCat}. Grey mice inherited *Tyr*^{CopyCat} but not *cas9*. White mice inherited both transgenes. **e**, A representative litter of five F_2 litters in which all offspring inherited *H11-cas9*. The mosaic mice also inherited *Tyr*^{CopyCat}.

Female *Rosa26-cas9;Tyr*$^{ch/ch}$ and *H11-cas9;Tyr*$^{ch/ch}$ mice were each crossed to *Tyr*$^{CopyCat/+}$ males to combine the gRNA and Cas9 protein in the early embryo (Fig. 1b). In absence of a loss-of-function mutation in exon 4 of the receiver chromosome, *Tyr*$^{CopyCat/ch}$ mice should appear grey (see *cas9*$^{-}$;*Tyr*$^{CopyCat/ch}$ mice in Fig. 1d). However, we did not observe any grey *cas9*$^{+}$;*Tyr*$^{CopyCat/ch}$ mice in the F_2 offspring of either cross. Instead, all 17 of the *Rosa26-cas9;Tyr*$^{CopyCat/ch}$ mice were entirely white. Among *H11-cas9;Tyr*$^{CopyCat/ch}$ mice, 21 of the F_2 progeny (87.5%) were a mosaic mixture of grey and white fur, and three mice (12.5%) were entirely white (Fig. 1d, e and Extended Data Table 1). The prevalence of mosaicism in the *H11-cas9* mice, compared to the all-white mice produced by *Rosa26-cas9*, suggests that there may be a difference in the level and/or timing of Cas9 expression driven by these two transgenes.

Our next goal was to determine what type of repair events (NHEJ mutations or gene conversions by HDR) were transmitted to the next generation. To assess inheritance in many offspring, we crossed each F_2 male *Rosa26-cas9;Tyr*$^{CopyCat/ch}$ and *H11-cas9;Tyr*$^{CopyCat/ch}$ mouse to multiple albino CD-1 females (Fig. 1c), which carry a loss-of-function point mutation in the *Tyr* exon 1 (*Tyr*^{c}, here designated as *Tyr*^{null})[11,17]. We then genotyped F_3 offspring of this cross by PCR and DNA sequencing of exon 5 to identify those that inherited the *Tyr*^{ch}-marked receiver chromosome (Supplementary Fig. 4). In the absence of gene conversion, effectively none of these chromosomes would be predicted to also carry the *Tyr*^{CopyCat} allele, because *Tyr* exons 4 and 5 are separated by only approximately 9.1 kb.

Tyr$^{ch/null}$ mice should appear grey because of the partial activity of the hypomorphic *Tyr*^{ch} allele. However, among F_3 offspring with this genotype, 100% in the *Rosa26-cas9* lineage and 90.4% in the *H11-cas9* lineage were completely white, indicating frequent transmission of a CRISPR–Cas9-induced loss-of-function mutation on the receiver chromosome and consistent with the primarily albino coat colour of the F_2 parents (Fig. 1c and Extended Data Tables 1, 2). If the induced null alleles resulted from inter-homologue HDR copying the *Tyr*^{CopyCat} allele from the donor to the *Tyr*^{ch}-marked receiver chromosome, these white animals should also express the fluorescent mCherry marker. However, in these experiments none of the F_3 offspring that inherited the receiver chromosome in either the *Rosa26-cas9* or *H11-cas9* lineages expressed mCherry. PCR amplification of *Tyr* exon 4 confirmed that the *Tyr*^{CopyCat} element was not present in white *Tyr*$^{ch/null}$ F_3 progeny (Extended Data Table 2).

The different propensities to yield a full albino or mosaic coat colour pattern in the F_2 generation of *Rosa26-cas9* and *H11-cas9* lineages were consistent with differences in the number of unique NHEJ mutations that we identified on receiver chromosomes in individuals of each genotype. Sequenced PCR products from *Rosa26-cas9;Tyr*^{CopyCat} F_2 tails—which are somatic tissues that consist of both ectodermal and mesodermal derivatives—and from individual F_3 outcross offspring (representing the germline) typically exhibited only two unique NHEJ mutations, suggesting that many of these Cas9-induced mutations may have been generated in embryos at the 2–4-cell stage (average 2.4 alleles among offspring of five families; Extended Data Fig. 2 and Extended Data Table 3). By contrast, *H11-cas9;Tyr*^{CopyCat} F_2 tails and F_3 offspring had significantly more unique NHEJ mutations (average 4.6 alleles in five families; two-tailed Student's *t*-test, $P = 0.041$), consistent with the hypothesis that Cas9 is expressed at a later embryonic stage and/or at lower levels in this lineage.

We considered two explanations for the observation that *Tyr*^{CopyCat} was not copied to the receiver chromosome in the early embryo. The first possibility is that homologous chromosomes are not aligned for inter-homologue HDR to repair DSBs. Second, the DNA repair machinery in somatic cells typically favours NHEJ over HDR[8,9]. A possible solution to overcome both potential obstacles is to restrict CRISPR–Cas9 activity to coincide with meiosis in the developing germline. During meiosis, recombination of the maternal and paternal genomes is initiated by the formation of DSBs that are repaired by exchanging regions of homologous chromosomes that are physically paired during meiosis I[18]. Indeed, the molecular mechanisms of NHEJ are actively repressed to favour HDR during meiosis in many species, including mice[19].

To test the hypothesis that CRISPR–Cas9 activity will convert a heterozygous active genetic element to homozygosity during meiosis, we designed a crossing scheme to initiate Cas9 expression during germline development in *Tyr*$^{CopyCat/ch}$ mice. As no currently available transgenic mice express Cas9 under direct control of a germline-specific

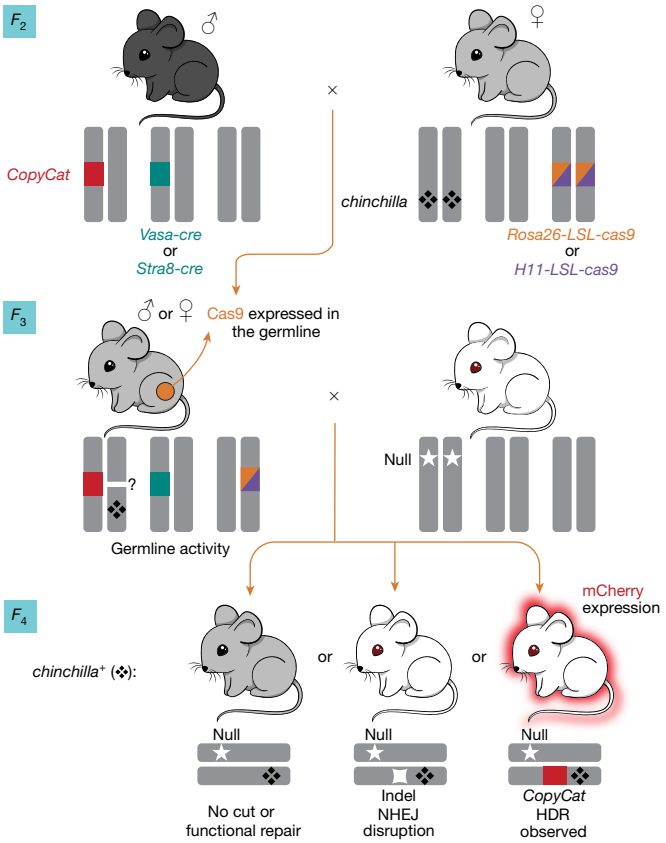

Fig. 2 | Breeding strategy to produce $Tyr^{CopyCat/ch}$ mice with a conditional *cas9* transgene and a germline restricted *cre* transgene. F_3 offspring were crossed to Tyr^{null} mice to assess F_4 phenotypes and genotypes. Quantification of observed outcomes in F_4 cross offspring are presented in Table 1.

promoter, we crossed mice with a conditional *Rosa26*- or *H11-LSL-cas9* transgene, each with a *loxP*-Stop-*loxP* (LSL) site preceding the Cas9 translation start site[15,16], to *Vasa-cre* (also known as *Ddx4-cre*) or *Stra8-cre* germline transgenic mice. *Vasa-cre* is expressed later than the endogenous *Vasa* transcript in both male and female germ cells[20], whereas *Stra8-cre* is limited to the male germline and is initiated in early-stage spermatogonia[21]. Although oogonia and spermatogonia are pre-meiotic, and spermatogonia are in fact mitotic, we reasoned that Cre protein must first accumulate before *cas9* can be expressed from the *LSL-cas9* conditional allele. The possible time delay may require initiation of *cre* expression before the onset of meiosis so that Cas9-induced DSBs can be resolved by inter-homologue HDR before segregation of homologous chromosomes at the end of meiosis I. We generated each combination of these *cre* and conditional *cas9* lines in case the timing or levels of Cas9 expression were critical variables in these crosses. We also assessed males and females of the *Vasa* strategies in case there were sex-dependent differences in animals that inherit the same genotype.

Males heterozygous for $Tyr^{CopyCat}$ and the *Vasa-cre* transgene were crossed to females homozygous for both the Tyr^{ch} allele and one of the two conditional *cas9* transgenes (Fig. 2). We avoided the reverse cross using female *Vasa-cre* mice, because Cre protein maternally deposited in the egg[20] might induce recombination of the conditional *cas9* allele and induce mutations in the early embryo similar to what we observed in the experiments using constitutive *cas9* transgenes. Introducing the *Vasa-cre* transgene by inheritance from the male instead resulted in most offspring that were entirely grey, owing to the $Tyr^{CopyCat/ch}$ genotype, and a few mosaic animals (Supplementary Table 4). The presence of mosaicism suggests that this conditional approach to restrict *cas9* expression to the germline resulted in some spurious cleavage of the *Tyr* locus in somatic tissues.

Table 1 | Observed F_4 outcomes of germline Cas9 strategies

cre	*cas9*	F_3 parent		No cut or functional repair	NHEJ disruption	HDR conversion	Observed HDR conversion (%)
Vasa	*Rosa26*	F	1	–	15	–	–
			2	1	2	–	–
			3	–	3	1	25
			4	4	5	3	25
			5	6	6	1	8
Vasa	*Rosa26*	M	1	–	25	–	–
			2	–	17	–	–
Vasa	*H11*	F	1	4	1	13	72
			2	10	7	4	19
			3	4	–	5	56
			4	8	4	4	25
			5	8	3	10	48
Vasa	*H11*	M	1	–	15	–	–
			2	–	5	–	–
			3	–	2	–	–
			4	–	3	–	–
Stra8	*Rosa26*	M	1	–	19	–	–
			2	–	3	–	–
Stra8	*H11*	M	1	3	21	–	–

F, female. M, male.

We first tested whether Cas9 in the female germline could promote copying of the $Tyr^{CopyCat}$ element onto the receiver chromosome by crossing F_3 female mice of each *Vasa-cre* lineage to CD-1 (Tyr^{null}) males. In each cross, we identified F_4 offspring that inherited the Tyr^{ch}-marked chromosome (Fig. 2). As in the crosses to assess the effects of embryonic *cas9* expression, we expected that $Tyr^{ch/null}$ mice without a loss-of-function mutation in exon 4 of the receiver chromosome would be grey. Mice with a CRISPR–Cas9-induced NHEJ mutation in exon 4 should be white. Mice carrying a CRISPR–Cas9-induced mutation that was repaired by inter-homologue HDR should not only be white, but also show expression of mCherry (red fluorescence) owing to transmission of the mCherry-marked $Tyr^{CopyCat}$ active genetic element.

Table 1 summarizes the results of these crosses that demonstrate gene conversion upon Cas9 expression in the female germline. In contrast to early embryonic expression of *cas9*, we observed that the $Tyr^{CopyCat}$ transgene was copied to the Tyr^{ch}-marked receiver chromosome in both *Vasa-cre;Rosa26-LSL-cas9* and *Vasa-cre;H11-LSL-cas9* lineages. However, the observed efficiency differed between genotypes; three out of five females of the *Vasa-cre;Rosa26-LSL-cas9* lineage and all five females of the *Vasa-cre;H11-LSL-cas9* lineage transmitted a Tyr^{ch}-marked chromosome that contained a $Tyr^{CopyCat}$ insertion to at least one offspring. Although there was considerable variation among females with the same genotype, the highest observed frequency of gene conversion (72.2%) within a germline produced 13 out of 18 Tyr^{ch} offspring with a $Tyr^{CopyCat}$ insertion in the *Vasa-cre;H11-LSL-cas9* lineage (Table 1 and Extended Data Table 4). The probability of obtaining an animal with this genotype by natural meiotic recombination mechanisms is very low (4.7×10^{-5}) owing to ultra-tight linkage between the $Tyr^{CopyCat}$ and Tyr^{ch} alleles. Although it seems probable that inter-homologue HDR of Cas9-induced DSBs uses the same DNA-repair machinery that is active during meiotic recombination, these copying events cannot be explained by an increased incidence of chromosomal crossover, because all animals that inherited the donor chromosome lacking the Tyr^{ch} marker expressed mCherry (Extended Data Table 4).

In contrast to the 41 copying events that we observed out of a total of 132 $Tyr^{ch/null}$ offspring of female mice, we observed no copying in a total of 113 offspring of males in which conditional *cas9* expression was induced by either *Vasa-cre* or *Stra8-cre* (Table 1 and Extended Data Table 4).

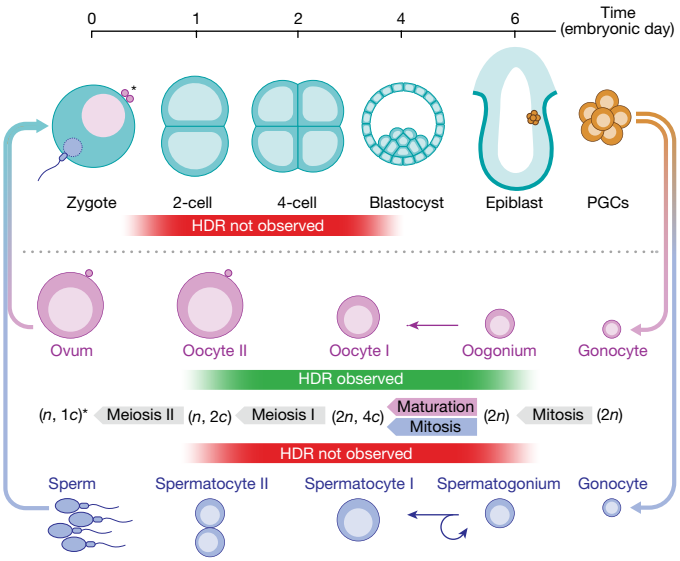

Fig. 3 | Gene conversion by an active genetic element was observed in the female germline and not in the male germline or in the early embryo. Schematic of early embryonic and male and female germline development overlaid with the presence or absence of observed HDR. PGCs, primordial germ cells; *n*, number of homologous chromosomes; *c*, chromosome copy number. The asterisk indicates the difference between male sperm (*n*, 1*c*) and female ovum, which remains (*n*, 2*c*) until second polar body extrusion after fertilization.

It is possible, however, that the number of families and of offspring in each family—which was limited by unexplained low male fertility—was insufficient to detect low-efficiency copying in each of four genetic strategies. If there is indeed a difference between males and females in the efficiency of $Tyr^{CopyCat}$ copying, we can consider two potential explanations. First, despite equivalent genotypes in the male and female *Vasa-cre* lineages, Cre, Cas9 and/or gRNA may not be well-expressed in the male germline. However, the high frequency of white $Tyr^{ch/null}$ offspring suggests that DSB formation is very efficient in males. Second, spermatogonia continually undergo mitosis and produce new primary spermatocytes throughout the life of a male in mammals[22]. By contrast, oogonia directly enlarge without further mitosis to form all of the primary oocytes in the embryo[23]. The difference in the observed efficiency of inter-homologue HDR between females and males at this locus may therefore reflect a requirement for the precise timing of CRISPR–Cas9 activity to coincide with meiosis (Fig. 3). NHEJ indels in males may result from DSB repair that occurs before the alignment of homologous chromosomes in meiosis I. Similarly, the higher observed efficiency of inter-homologue HDR in females of the *H11-LSL-cas9* conditional strategy may relate to the lower or delayed *cas9* expression from the *H11* locus, compared to *Rosa26*, which was evident in the constitutive crosses (Fig. 1d, e and Extended Data Tables 1, 3). Thus, in the *Vasa-cre;H11-LSL-cas9* mice, DSB formation may have been fortuitously delayed to fall within a more optimal window during female meiosis.

In summary, we demonstrate that the fundamental mechanism of a CRISPR–Cas9-mediated gene drive is feasible in mice. However, our comparison of eight different genetic strategies indicates that the precise timing of Cas9 expression may present a greater challenge in rodents than in insects to restrict DSB formation to a window when breaks can be efficiently repaired by the endogenous meiotic recombination machinery. These data are therefore critical to the ongoing discussion about whether CRISPR–Cas9-mediated gene drives could be used to reduce invasive rodent populations, because it appears that both the optimism and concerns are likely to be premature. Further optimization to increase the frequency of gene conversion in both males and females and to reduce the prevalence of drive-resistant alleles (NHEJ indels that alter the gRNA target site) would be necessary to achieve rapid and sustained suppression of wild populations[24–29].

Nevertheless, the copying efficiencies that we observed here would be more than sufficient for a broad range of laboratory applications. For example, the average observed copying rate of 44% using the most efficient genetic strategy in females (*Vasa-cre;H11-LSL-cas9*) combined ultra-tightly linked tyrosinase mutations such that 22.5% of all offspring inherited a chromosome with both alleles, which would not be possible through Mendelian inheritance. This observed average copying rate would also be expected to increase the inheritance of a single desired allele from 50% to 72%, and the highest rate of gene conversion that we observed (72.2%) would result in an 86% frequency of transmitting a desired allele. If multiple genes could be simultaneously converted to homozygosity, such high transmission frequencies that bypass the onerous constraint of genetic linkage stand to greatly accelerate the production of rodent models for a variety of complex genetic traits.

Online content

Any methods, additional references, Nature Research reporting summaries, source data, statements of data availability and associated accession codes are available at https://doi.org/10.1038/s41586-019-0875-2.

Received: 4 July 2018; Accepted: 7 December 2018;
Published online: 23 January 2019

1. Gantz, V. M. & Bier, E. The mutagenic chain reaction: a method for converting heterozygous to homozygous mutations. *Science* **348**, 442–444 (2015).
2. Gantz, V. M. et al. Highly efficient Cas9-mediated gene drive for population modification of the malaria vector mosquito *Anopheles stephensi*. *Proc. Natl Acad. Sci. USA* **112**, E6736–E6743 (2015).
3. Hammond, A. et al. A CRISPR–Cas9 gene drive system targeting female reproduction in the malaria mosquito vector *Anopheles gambiae*. *Nat. Biotechnol.* **34**, 78–83 (2016).
4. Kyrou, K. et al. A CRISPR–Cas9 gene drive targeting *doublesex* causes complete population suppression in caged *Anopheles gambiae* mosquitoes. *Nat. Biotechnol.* **36**, 1062–1066 (2018).
5. Gantz, V. M. & Bier, E. The dawn of active genetics. *BioEssays* **38**, 50–63 (2016).
6. Gould, F. Broadening the application of evolutionarily based genetic pest management. *Evolution* **62**, 500–510 (2008).
7. Esvelt, K. M., Smidler, A. L., Catteruccia, F. & Church, G. M. Emerging technology: concerning RNA-guided gene drives for the alteration of wild populations. *eLife* **3**, e03401 (2014).
8. Mao, Z., Bozzella, M., Seluanov, A. & Gorbunova, V. Comparison of nonhomologous end joining and homologous recombination in human cells. *DNA Repair (Amst.)* **7**, 1765–1771 (2008).
9. Miyaoka, Y. et al. Systematic quantification of HDR and NHEJ reveals effects of locus, nuclease, and cell type on genome-editing. *Sci. Rep.* **6**, 23549 (2016).
10. Xu, X.-R. S., Gantz, V. M., Siomava, N. & Bier, E. CRISPR/Cas9 and active genetics-based trans-species replacement of the endogenous *Drosophila kni*-L2 CRM reveals unexpected complexity. *eLife* **6**, e30281 (2017).
11. Yokoyama, T. et al. Conserved cysteine to serine mutation in tyrosinase is responsible for the classical albino mutation in laboratory mice. *Nucleic Acids Res.* **18**, 7293–7298 (1990).
12. Yen, S.-T. et al. Somatic mosaicism and allele complexity induced by CRISPR/Cas9 RNA injections in mouse zygotes. *Dev. Biol.* **393**, 3–9 (2014).
13. Miyagishi, M. & Taira, K. U6 promoter-driven siRNAs with four uridine 3′ overhangs efficiently suppress targeted gene expression in mammalian cells. *Nat. Biotechnol.* **20**, 497–500 (2002).
14. Boshart, M. et al. A very strong enhancer is located upstream of an immediate early gene of human cytomegalovirus. *Cell* **41**, 521–530 (1985).
15. Platt, R. J. et al. CRISPR–Cas9 knockin mice for genome editing and cancer modeling. *Cell* **159**, 440–455 (2014).
16. Chiou, S.-H. et al. Pancreatic cancer modeling using retrograde viral vector delivery and in vivo CRISPR/Cas9-mediated somatic genome editing. *Genes Dev.* **29**, 1576–1585 (2015).
17. Beermann, F. et al. Rescue of the albino phenotype by introduction of a functional tyrosinase gene into mice. *EMBO J.* **9**, 2819–2826 (1990).
18. Keeney, S., Giroux, C. N. & Kleckner, N. Meiosis-specific DNA double-strand breaks are catalyzed by Spo11, a member of a widely conserved protein family. *Cell* **88**, 375–384 (1997).
19. Goedecke, W., Eijpe, M., Offenberg, H. H., van Aalderen, M. & Heyting, C. Mre11 and Ku70 interact in somatic cells, but are differentially expressed in early meiosis. *Nat. Genet.* **23**, 194–198 (1999).
20. Gallardo, T., Shirley, L., John, G. B. & Castrillon, D. H. Generation of a germ cell-specific mouse transgenic Cre line, *Vasa-cre*. *Genesis* **45**, 413–417 (2007).
21. Sadate-Ngatchou, P. I., Payne, C. J., Dearth, A. T. & Braun, R. E. Cre recombinase activity specific to postnatal, premeiotic male germ cells in transgenic mice. *Genesis* **46**, 738–742 (2008).

22. de Rooij, D. G. & Grootegoed, J. A. Spermatogonial stem cells. *Curr. Opin. Cell Biol.* **10**, 694–701 (1998).
23. Pepling, M. E. From primordial germ cell to primordial follicle: mammalian female germ cell development. *Genesis* **44**, 622–632 (2006).
24. Burt, A. Site-specific selfish genes as tools for the control and genetic engineering of natural populations. *Proc. R. Soc. Lond. B* **270**, 921–928 (2003).
25. Deredec, A., Burt, A. & Godfray, H. C. J. The population genetics of using homing endonuclease genes in vector and pest management. *Genetics* **179**, 2013–2026 (2008).
26. Unckless, R. L., Clark, A. G. & Messer, P. W. Evolution of resistance against CRISPR/Cas9 gene drive. *Genetics* **205**, 827–841 (2017).
27. Noble, C., Olejarz, J., Esvelt, K. M., Church, G. M. & Nowak, M. A. Evolutionary dynamics of CRISPR gene drives. *Sci. Adv.* **3**, e1601964 (2017).
28. Marshall, J. M., Buchman, A., Sánchez C, H. M. & Akbari, O. S. Overcoming evolved resistance to population-suppressing homing-based gene drives. *Sci. Rep.* **7**, 3776 (2017).
29. Noble, C., Adlam, B., Church, G. M., Esvelt, K. M. & Nowak, M. A. Current CRISPR gene drive systems are likely to be highly invasive in wild populations. *eLife* **7**, e33423 (2018).

Acknowledgements We thank K. Hanley for the DNA extraction protocol; A. Green and A.-C. Chen for genotyping assistance; M. Tran for laser-capture microdissection in an effort to genotype spermatogonia; P. Jain for assistance with fibroblast transfection; H. Cook-Andersen and M. Wilkinson for conversations about mouse germline development; L. Montoliu for discussion of the tyrosinase locus; M. Tuszynski for plasmids and for early support of the project. This work was funded by a Searle Scholar Award from the Kinship Foundation, a Pew Biomedical Scholar Award from the Pew Charitable Trusts, a Packard Fellowship in Science and Engineering from the David and Lucile Packard Foundation, and NIH grant R21GM129448 awarded to K.L.C. E.B. was supported by NIH grant R01GM117321, a Paul G. Allen Frontiers Group Distinguished Investigators Award and a gift from the Tata Trusts in India to TIGS-UCSD and TIGS-India. H.A.G. was supported by a Ruth Stern Graduate Fellowship and by the NIH Cell and Molecular Genetics training grant T32GM724039; V.M.G. was supported by NIH grant DP5OD023098.

Reviewer information *Nature* thanks B. Conklin, S. Qi and the other anonymous reviewer(s) for their contribution to the peer review of this work.

Author contributions H.A.G., V.M.G., G.P., E.B. and K.L.C. conceived and designed the research; V.M.G. and G.P. designed and cloned the $Tyr^{CopyCat}$ transgene and validated mCherry expression in vitro; X.-R.S.X. validated *Tyr4a* gRNA cleavage activity in vitro; H.A.G. and K.L.C. designed the breeding strategies; H.A.G. acquired and established mouse lines, developed genotyping protocols, and conducted mouse breeding, phenotyping and genotyping; H.A.G. curated the data and analyses; K.L.C. and E.B. supervised the research; K.L.C. wrote the original draft; H.A.G., V.M.G., E.B. and K.L.C. revised subsequent drafts.

Competing interests V.M.G., E.B. and K.L.C. hold advisory board positions with Synbal. All other authors declare that they have no competing interests.

Additional information
Extended data is available for this paper at https://doi.org/10.1038/s41586-019-0875-2.
Supplementary information is available for this paper at https://doi.org/10.1038/s41586-019-0875-2.
Reprints and permissions information is available at http://www.nature.com/reprints.
Correspondence and requests for materials should be addressed to K.L.C.
Publisher's note: Springer Nature remains neutral with regard to jurisdictional claims in published maps and institutional affiliations.

METHODS

Statistics and reproducibility. The five families in each of the constitutive crosses (Extended Data Table 2) are considered five independent experiments with each F_3 offspring representing an early embryonic DSB repair event in the F_2 parent. Each F_4 offspring in Extended Data Table 4 represents a germline DSB repair event, an independent data point and each family is considered an independent trial. No statistical method was used to predetermine sample size. Given breeding limitations, we assessed as many offspring as possible in each family and aimed to assess up to five families for each strategy. To detect gene conversion events, we used genetic linkage rather than a statistical test of inheritance greater than 50% expected by Mendelian segregation. Specifically, the receiver chromosome was marked with a SNP (Tyr^{ch}) located approximately 9.1 kb from the target site for gene conversion. The probability of a naturally occurring recombination event that would unite these ultra-tightly linked loci on the same chromosome is 4.7×10^{-5}, because the average genetic distance[30] for mouse chromosome 7 is 0.52 cM Mb^{-1}.

Reporting summary. Further information on research design is available in the Nature Research Reporting Summary linked to this paper.

Data availability

All genotyping data for F_3 offspring of constitutive crosses and F_4 offspring of germline conditional crosses is available at Zenodo with the identifier https://doi.org/10.5281/zenodo.2003087. Annotated sequence data for the $Tyr^{CopyCat}$ transgene is available in GenBank with the accession number MK160997.

30. Jensen-Seaman, M. I. et al. Comparative recombination rates in the rat, mouse, and human genomes. *Genome Res.* **14**, 528–538 (2004).

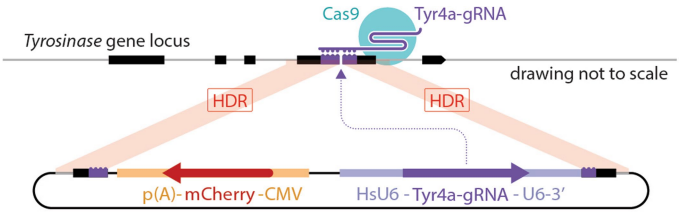

Extended Data Fig. 1 | Knock-in strategy using the *Tyr*^{CopyCat}-targeting vector. The U6-Tyr4a gRNA (tyrosinase exon 4 gRNA a) and CMV-mCherry were inserted into the cut site of the *Tyr4a* gRNA by HDR after CRISPR–Cas9 DSB formation targeted by the *Tyr4a* gRNA. See Supplementary Methods and Supplementary Figs. 1, 2 for additional details.

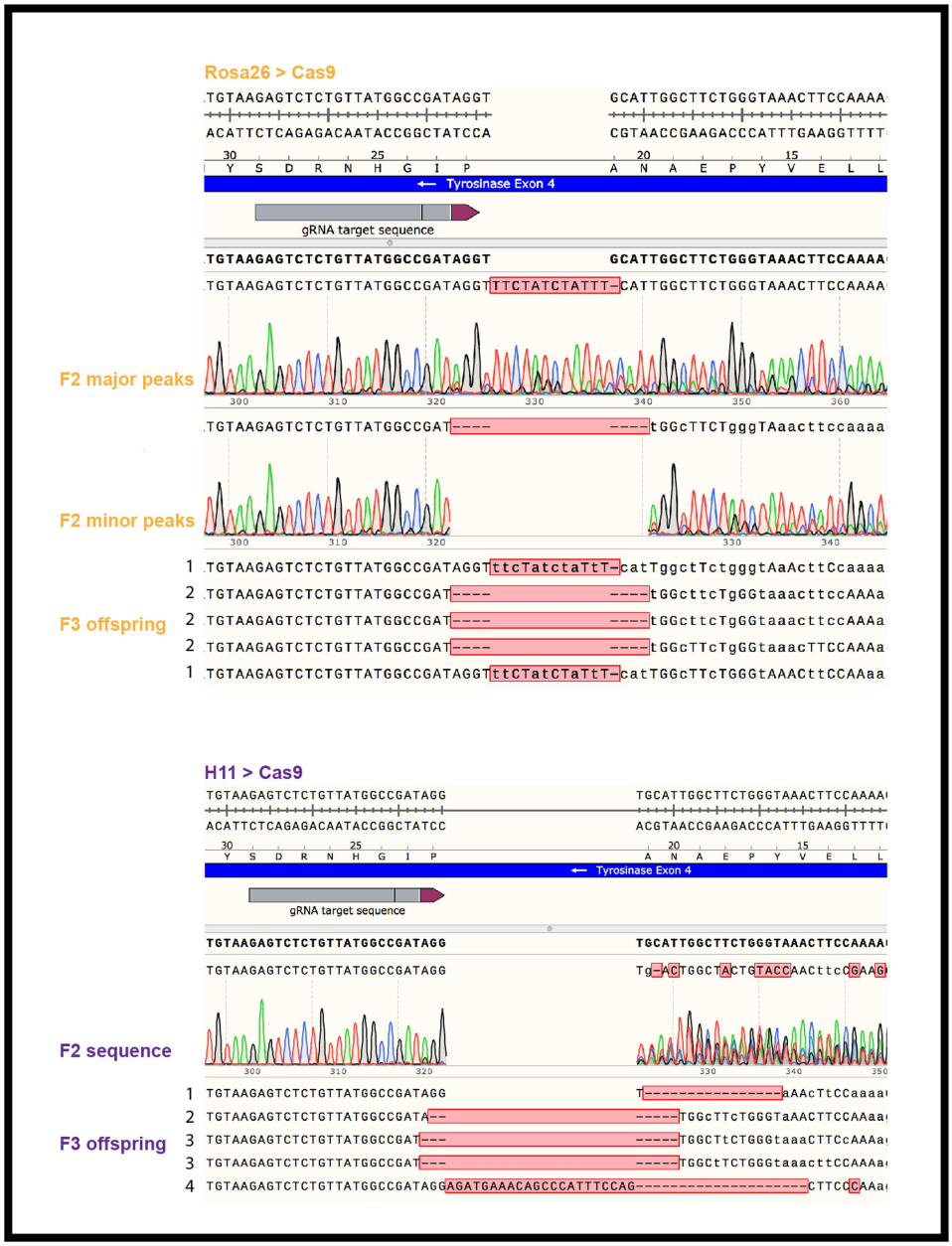

Extended Data Fig. 2 | *Rosa26-cas9* and *H11-cas9* constitutive lineages have different numbers of unique NHEJ indels. Sanger sequencing of the *Tyr4a* gRNA target exon amplified from tail-tip genomic DNA using TyrHALF2 and TyrHARR2 primers as specified in Supplementary Table 3. Top, a single representative Sanger sequence trace of the bulk PCR product amplified from a *Rosa26-cas9*;$Tyr^{CopyCat}$-positive F_2 mouse (*Rosa26* family 1 in Extended Data Table 3) with either major or minor peaks called revealing two distinct alleles. Five Tyr^{ch}-positive F_3 offspring of this F_2 individual each match one of the two alleles (marked 1 (insertion) and 2 (deletion)). Bottom, a single representative sequence trace of the bulk PCR product amplified from an *H11-cas9*;$Tyr^{CopyCat}$-positive F_2 mouse (*H11* family 1 in Extended Data Table 3). Alternate alleles cannot be called because of the complexity of overlapping peaks. Five Tyr^{ch}-positive F_3 offspring each have one of four different alleles (marked 1, 2, 3 and 4). Sequence trace data are representative of all 90 individuals of 5 families of each constitutive strategy described in Extended Data Table 3.

Extended Data Table 1 | Coat colour of F_2 individuals that were constitutive *cas9*-positive and $Tyr^{CopyCat/ch}$

	Rosa26>Cas9	H11>Cas9
White	17	3
Mosaic	0	21

Extended Data Table 2 | Analyses of phenotypes and genotypes of all F_3 progeny of the constitutive *cas9* crosses

			Chinchilla + F3 offspring			
	F2 parent color	Total F3 Chinchilla-	Total F3 Chinchilla+	White (NHEJ mutation)	Grey (no cut or functional repair)	mCherry+ (HDR gene conversion)
Rosa26 Family 1	white	30	20	20	0	0
Rosa26 Family 2	white	11	15	15	0	0
Rosa26 Family 3*	white	28*	16	16	0	0
Rosa26 Family 4	white	22	22	22	0	0
Rosa26 Family 5	white	16	16	16	0	0
H11 Family 1	prim. white mosaic	14	15	15	0	0
H11 Family 2	prim. grey mosaic	23	28	25	3	0
H11 Family 3	prim. white mosaic	13	9	9	0	0
H11 Family 4	prim. white mosaic	12	15	15	0	0
H11 Family 5	mosaic	23	24	18	6	0

Genotypes and phenotypes of all F_3 progeny in Fig. 1c that are the offspring of a subset of F_2 individuals listed in Extended Data Table 1. Prim., primarily; referring to the coat colour that covers the greatest total area when there was obviously not an equal proportion of white and grey.
*A family with offspring that were Tyr^{ch}-negative and mCherry-negative, suggesting a large deletion in the recipient chromosome that may encompass the Tyr^{ch} SNP.

Extended Data Table 3 | Allelic complexity of the constitutive Rosa26- and *H11-cas9* families

	Number of distinct NHEJ alleles in 'n' *Tyr*^{chinchilla}+ offspring
Rosa26 Family 1	2 (n=9)
Rosa26 Family 2	3 (n=10)
Rosa26 Family 3*	2 (n=9)
Rosa26 Family 4	2 (n=7)
Rosa26 Family 5	3 (n=13)
H11 Family 1	4 (n=10)
H11 Family 2	6 (n=9)
H11 Family 3	4 (n=6)
H11 Family 4	2 (n=8)
H11 Family 5	7 (n=9)

*A family with offspring that were *Tyr*^{ch}-negative and mCherry-negative, suggesting a large deletion in the recipient chromosome that may encompass the *Tyr*^{ch} SNP. This was counted as one of the two unique NHEJ indels.

Extended Data Table 4 | Analyses of phenotypes and genotypes of all F_4 progeny of the germline Cas9 crosses

Vasa>Cre
Rosa26>LSL Cas9

Female

	F3 parent color	Chinchilla – mCherry + F4 Total	Chinchilla + F4 offspring: Chinchilla + F4 Total	White, mCherry - (NHEJ mutation)	Mosaic (variable NHEJ mutations)	Grey (no cut or functional repair)	White, mCherry + (HDR conversion)	% Copying in F3 germline
Rosa26 Family 1	mosaic	10	15	14	1	0	0	0.0
Rosa26 Family 2	grey	8	3	1	1	1	0	0.0
Rosa26 Family 3	mosaic	6	4	3	0	0	1	25.0
Rosa26 Family 4	grey	9	12	2	3	4	3	25.0
Rosa26 Family 5	grey	14	13	6	0	6	1	7.7

Male

	F3 parent color	Chinchilla – mCherry + F4 Total	Chinchilla + F4 offspring: Chinchilla + F4 Total	White, mCherry - (NHEJ mutation)	Mosaic (variable NHEJ mutations)	Grey (no cut or functional repair)	White, mCherry + (HDR conversion)	% Copying in F3 germline
Rosa26 Family 1	grey	30	25	25	0	0	0	0.0
Rosa26 Family 2	grey	19	17	17	0	0	0	0.0

Vasa>Cre
H11>LSL Cas9

Female

	F3 parent color	Chinchilla – mCherry + F4 Total	Chinchilla + F4 offspring: Chinchilla + F4 Total	White, mCherry - (NHEJ mutation)	Mosaic (variable NHEJ mutations)	Grey (no cut or functional repair)	White, mCherry + (HDR conversion)	% Copying in F3 germline
H11 Family 1	grey	17	18	0	1	4	13	72.2
H11 Family 2	grey	18	21	5	2	10	4	19.0
H11 Family 3	grey	13	9	0	0	4	5	55.6
H11 Family 4	grey	14	16	2	2	8	4	25.0
H11 Family 5	grey	13	21	2	1	8	10	47.6

Male

	F3 parent color	Chinchilla – mCherry + F4 Total	Chinchilla + F4 offspring: Chinchilla + F4 Total	White, mCherry - (NHEJ mutation)	Mosaic (variable NHEJ mutations)	Grey (no cut or functional repair)	White, mCherry + (HDR conversion)	% Copying in F3 germline
H11 Family 1	grey	33	15	15	0	0	0	0.0
H11 Family 2	grey	9	5	5	0	0	0	0.0
H11 Family 3	grey	2	2	2	0	0	0	0.0
H11 Family 4	grey	2	3	3	0	0	0	0.0

Stra8>Cre

Rosa26>LSL Cas9
Male

	F3 parent color	Chinchilla – mCherry + F4 Total	Chinchilla + F4 offspring: Chinchilla + F4 Total	White, mCherry - (NHEJ mutation)	Mosaic (variable NHEJ mutations)	Grey (no cut or functional repair)	White, mCherry + (HDR conversion)	% Copying in F3 germline
Rosa26 Family 1	grey	23	19	19	0	0	0	0.0
Rosa26 Family 2	grey	3	3	3	0	0	0	0.0

H11>LSL Cas9
Male

	F3 parent color	Chinchilla – mCherry + F4 Total	Chinchilla + F4 offspring: Chinchilla + F4 Total	White, mCherry - (NHEJ mutation)	Mosaic (variable NHEJ mutations)	Grey (no cut or functional repair)	White, mCherry + (HDR conversion)	% Copying in F3 germline
H11 Family 1	grey	22	24	21	0	3	0	0.0

Phenotypes and genotypes of all F_4 progeny that are the offspring of a subset of F_3 individuals listed in Supplementary Table 4.

nature research

Corresponding author(s): Kimberly L. Cooper

Reporting Summary

Nature Research wishes to improve the reproducibility of the work that we publish. This form provides structure for consistency and transparency in reporting. For further information on Nature Research policies, see Authors & Referees and the Editorial Policy Checklist.

Statistical parameters

When statistical analyses are reported, confirm that the following items are present in the relevant location (e.g. figure legend, table legend, main text, or Methods section).

n/a	Confirmed	
☐	☒	The exact sample size (*n*) for each experimental group/condition, given as a discrete number and unit of measurement
☐	☒	An indication of whether measurements were taken from distinct samples or whether the same sample was measured repeatedly
☐	☒	The statistical test(s) used AND whether they are one- or two-sided *Only common tests should be described solely by name; describe more complex techniques in the Methods section.*
☒	☐	A description of all covariates tested
☒	☐	A description of any assumptions or corrections, such as tests of normality and adjustment for multiple comparisons
☒	☐	A full description of the statistics including central tendency (e.g. means) or other basic estimates (e.g. regression coefficient) AND variation (e.g. standard deviation) or associated estimates of uncertainty (e.g. confidence intervals)
☒	☐	For null hypothesis testing, the test statistic (e.g. *F*, *t*, *r*) with confidence intervals, effect sizes, degrees of freedom and *P* value noted *Give P values as exact values whenever suitable.*
☒	☐	For Bayesian analysis, information on the choice of priors and Markov chain Monte Carlo settings
☒	☐	For hierarchical and complex designs, identification of the appropriate level for tests and full reporting of outcomes
☒	☐	Estimates of effect sizes (e.g. Cohen's *d*, Pearson's *r*), indicating how they were calculated
☒	☐	Clearly defined error bars *State explicitly what error bars represent (e.g. SD, SE, CI)*

Our web collection on statistics for biologists may be useful.

Software and code

Policy information about availability of computer code

Data collection	No software was used in this analysis
Data analysis	We used SnapGene for designing the targeting constructs and for analyzing Sanger sequencing data.

For manuscripts utilizing custom algorithms or software that are central to the research but not yet described in published literature, software must be made available to editors/reviewers upon request. We strongly encourage code deposition in a community repository (e.g. GitHub). See the Nature Research guidelines for submitting code & software for further information.

Data

Policy information about availability of data

All manuscripts must include a data availability statement. This statement should provide the following information, where applicable:

- Accession codes, unique identifiers, or web links for publicly available datasets
- A list of figures that have associated raw data
- A description of any restrictions on data availability

All data is available in the main text or the supplementary materials. Primary genotyping data is being currated and will be deposited to Figshare.

Field-specific reporting

Please select the best fit for your research. If you are not sure, read the appropriate sections before making your selection.

☒ Life sciences ☐ Behavioural & social sciences ☐ Ecological, evolutionary & environmental sciences

For a reference copy of the document with all sections, see nature.com/authors/policies/ReportingSummary-flat.pdf

Life sciences study design

All studies must disclose on these points even when the disclosure is negative.

Sample size	Given the ultra-tight genetic linkage of the Tyr^Ch marker and the Tyr^CopyCat active genetic element, the probability of natural recombination between these alleles is 4.7x10-5. We include this information in "Statistics and Reproducibility."
Data exclusions	No data were excluded from these results
Replication	Copying of the "CopyCat" element was confirmed by PCR twice from the same sample and again from a separate tissue collected from the same individual. Copying was also evident in multiple animals that were the product of multiple different mating pairs.
Randomization	This study did not include multiple treatment conditions, and therefore random assignment was not necessary. All pups available were analyzed; no random sampling of offspring was necessary.
Blinding	Investigators had no knowledge of phenotype (presence/absence of mCherry, coat color) when performing PCR or Sanger sequencing to assess genotype.

Reporting for specific materials, systems and methods

Materials & experimental systems

n/a	Involved in the study
☐	☒ Unique biological materials
☒	☐ Antibodies
☒	☐ Eukaryotic cell lines
☒	☐ Palaeontology
☐	☒ Animals and other organisms
☒	☐ Human research participants

Methods

n/a	Involved in the study
☒	☐ ChIP-seq
☒	☐ Flow cytometry
☒	☐ MRI-based neuroimaging

Unique biological materials

Policy information about availability of materials

Obtaining unique materials	The "CopyCat" mouse used in this study is a unique transgenic animal. Production of this mouse is detailed in the methods section. Individuals of this mouse line may be available upon request from the corresponding author.

Animals and other organisms

Policy information about studies involving animals; ARRIVE guidelines recommended for reporting animal research

Laboratory animals	Laboratory mice (Mus musculus) were used in this study. The following backgrounds were used: CD-1, FVB, C57B6|J. The following specific strains were used: "CopyCat" (transgenic mouse produced for this study), Jackson lab strains #26175, 26179, 26816, 27650, 17490, 6954, 4828. Adult animals were used for breeding, and genotyping was performed from birth to P21.
Wild animals	No wild animals were used in this study.
Field-collected samples	No field collected samples were used in this study.